

New Nitrosyl Derivatives of Diiron Dithiolates Related to the Active Site of the [FeFe]-Hydrogenases

Matthew T. Olsen, Aaron K. Justice, Frédéric Gloaguen, Thomas B. Rauchfuss,* and Scott R. Wilson

Department of Chemistry, University of Illinois, Urbana, Illinois 61801

Received August 12, 2008

Nitrosyl derivatives of diiron dithiolato carbonyls have been prepared starting from the precursor $\text{Fe}_2(\text{S}_2\text{C}_n\text{H}_{2n})(\text{dppv})(\text{CO})_4$ (dppv = *cis*-1,2-bis(diphenylphosphinoethylene)). These studies expand the range of substituted diiron(I) dithiolato carbonyl complexes. From $[\text{Fe}_2(\text{S}_2\text{C}_2\text{H}_4)(\text{CO})_3(\text{dppv})(\text{NO})]\text{BF}_4$ ($[\text{1}(\text{CO})_3]\text{BF}_4$), the following compounds were prepared: $[\text{1}(\text{CO})_2(\text{PMe}_3)]\text{BF}_4$, $[\text{1}(\text{CO})(\text{dppv})]\text{BF}_4$, $\text{NEt}_4[\text{1}(\text{CO})(\text{CN})_2]$, and $\text{1}(\text{CO})(\text{CN})(\text{PMe}_3)$. Some of these substitution reactions occur via the addition of 2 equiv of the nucleophile followed by the dissociation of one nucleophile and decarbonylation. Such a double adduct was characterized crystallographically in the case of $[\text{Fe}_2(\text{S}_2\text{C}_2\text{H}_4)(\text{CO})_3(\text{dppv})(\text{NO})(\text{PMe}_3)_2]\text{BF}_4$. This result shows that the addition of two ligands causes scission of the Fe–Fe bond and one Fe–S bond. When cyanide is the nucleophile, nitrosyl migrates away from the Fe(dppv) site, yielding a $\text{Fe}(\text{CN})_2(\text{NO})$ derivative. Compounds $[\text{1}(\text{CO})_3]\text{BF}_4$, $[\text{1}(\text{CO})_2(\text{PMe}_3)]\text{BF}_4$, and $[\text{1}(\text{CO})(\text{dppv})]\text{BF}_4$ were also prepared by the addition of NO^+ to the di-, tri-, and tetrasubstituted precursors. In these cases, the NO^+ appears to form an initial $36e^-$ adduct containing terminal Fe–NO, followed by decarbonylation. Several complexes were prepared by the addition of NO to the mixed-valence Fe(I)Fe(II) derivatives. The diiron nitrosyl complexes reduce at mild potentials and in certain cases form weak adducts with CO. IR and EPR spectra of $\text{1}(\text{CO})(\text{dppv})$, generated by low-temperature reduction of $[\text{1}(\text{CO})(\text{dppv})]\text{BF}_4$ with $\text{Co}(\text{C}_5\text{Me}_5)_2$, indicates that the SOMO is located on the FeNO subunit.

Introduction

The substitution chemistry for compounds of the type $[\text{Fe}_2(\text{SR})_2(\text{CO})_{6-x}\text{L}_x]^z$ is well-developed for L = tertiary phosphines and cyanide.¹ These synthetic transformations were mainly developed en route to functional and structural mimics of the active site of the [FeFe]-hydrogenase enzymes. The enzymes catalyze the redox interconversion of protons and H_2 and do so at near-thermodynamic potentials.² The high efficiency of the Fe-based catalysts has motivated numerous studies on the synthesis and reactivity of diiron dithiolato carbonyls.

Recently, we reported a series of diiron dithiolate– PMe_3 complexes containing nitrosyl ligands. These compounds are of interest because they adopt “rotated” structures as seen in related mixed-valence $\text{Fe}^{\text{I}}\text{Fe}^{\text{II}}$ complexes, the so-called H_{ox}

models.³ Associated with their distinctive structure, these nitrosyl compounds are Lewis acidic, which is unknown for other $[\text{Fe}^{\text{I}}]_2$ species but characteristic of the mixed valence H_{ox} state and its models. Our results indicated the likely stability of other nitrosyl complexes. We therefore have investigated the nitrosyl derivatives of the diiron(I) dithiolates supported by *cis*-1,2-bis(diphenylphosphinoethylene) (dppv). For studying the fundamental reactivity of diiron(I) dithiolates, we have shown that $\text{Fe}_2(\text{S}_2\text{C}_n\text{H}_{2n})(\text{CO})_4(\text{dppv})$ ($n = 2, 3$) are useful reagents because of their high reactivity and the simplified structures of the products.⁴ We expected, incorrectly that NO^+ would yield highly polar derivatives of $\text{Fe}_2(\text{S}_2\text{C}_n\text{H}_{2n})(\text{CO})_4(\text{dppv})$.

Nitrosyl derivatives of iron thiolates are of course well-known. The first synthetic iron-sulfide cluster, Roussin’s Red anion, $[\text{Fe}_2\text{S}_2(\text{NO})_4]^{2-}$, led to the corresponding “esters”, $\text{Fe}_2(\text{SR})_2(\text{NO})_4$ (R = alkyl, aryl).⁵ The Roussin esters have come under renewed scrutiny because of their connection

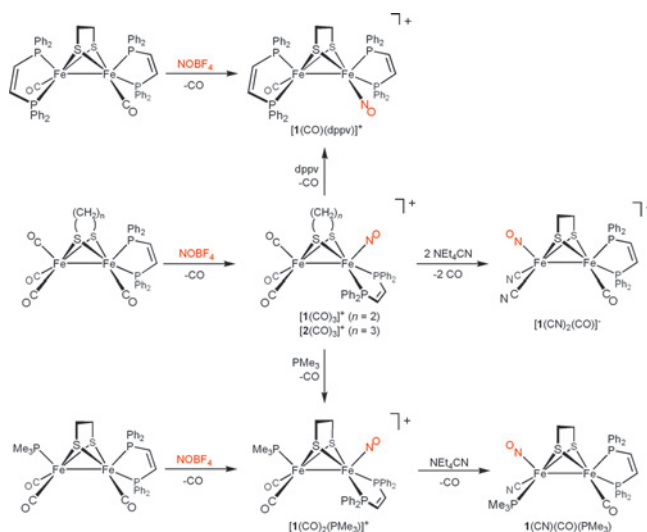
* Author to whom correspondence should be addressed. E-mail: rauchfuz@uiuc.edu.

- (1) Liu, X.; Ibrahim, S. K.; Tard, C.; Pickett, C. J. *Coord. Chem. Rev.* **2005**, *249*, 1641–1652. Mejia-Rodriguez, R.; Chong, D.; Reibenspies, J. H.; Soriaga, M. P.; Darensbourg, M. Y. *J. Am. Chem. Soc.* **2004**, *126*, 12004–12014. Zhao, X.; Georgakaki, I. P.; Miller, M. L.; Yarbrough, J. C.; Darensbourg, M. Y. *J. Am. Chem. Soc.* **2001**, *123*, 9710–9711.
- (2) Vincent, K. A.; Parkin, A.; Armstrong, F. A. *Chem. Rev.* **2007**, *107*, 4366–4413.

- (3) Liu, T.; Darensbourg, M. Y. *J. Am. Chem. Soc.* **2007**, *129*, 7008–9. Justice, A. K.; Rauchfuss, T. B.; Wilson, S. R. *Angew. Chem., Int. Ed.* **2007**, *46*, 6152–6154.

- (4) Justice, A. K.; Zampella, G.; De Gioia, L.; Rauchfuss, T. B.; van der Vlugt, J. I.; Wilson, S. R. *Inorg. Chem.* **2007**, *46*, 1655–1664.

- (5) Butler, A. R.; Megson, I. L. *Chem. Rev.* **2002**, *102*, 1155–1165.

Scheme 1. Diiron Dithiolato Nitrosyl Complexes Described in This Work

to the so-called dinitrosyl iron complexes.⁶ Nitric oxide inhibits [NiFe] hydrogenases,⁷ although the reactivity of NO with [FeFe] hydrogenases has not been reported.

Both NO and NO⁺ are electrophiles;⁸ hence, it is worth mentioning the reactivity of other electrophiles with Fe₂(SR)₂(CO)_{6-x}L_x. Substituted diiron(I) dithiolates protonate readily.⁹ Sources of SME⁺,¹⁰ Br⁺, I⁺,¹¹ and HgCl⁺¹² have long been known to add across the Fe–Fe bond.

Results

[Fe₂(S₂C_nH_{2n})(CO)₃(dppv)(NO)]⁺ (*n* = 2, 3). The salts [Fe₂(S₂C_nH_{2n})(NO)(CO)₃(dppv)]BF₄ (*n* = 2, [1(CO)₃]BF₄; *n* = 3, [2(CO)₃]BF₄) were found to form efficiently upon treatment of CH₂Cl₂ solutions of Fe₂(S₂C_nH_{2n})(CO)₄(dppv) with NOBF₄ at 20 °C (Scheme 1). Indicative of their high electrophilicity, both [1(CO)₃]BF₄ and [2(CO)₃]BF₄ exhibit limited stability in MeCN solutions at room temperature, although CH₂Cl₂ and tetrahydrofuran solutions are stable for hours. These mononitrosyl complexes were unreactive toward additional equivalents of NOBF₄ at room temperature.

The crystallographically determined structure of [2(CO)₃]BF₄ revealed that the nitrosyl ligand is apical, the cation having idealized C_s symmetry (Figure 1). The complex exhibits a slight twisting distortion in both the Fe(dp-

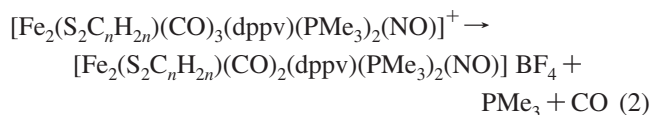
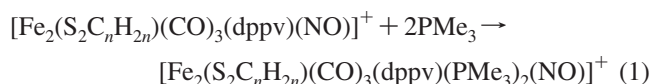
pv)(NO)⁺ and Fe(CO)₃ subunits, reminiscent of the structure seen for [Fe₂(S₂C_nH_{2n})(CO)₃(PMe₃)₂(NO)]⁺.¹³

In addition to the ν_{NO} band at 1796 cm⁻¹, the IR spectrum of [1(CO)₃]BF₄ features two ν_{CO} bands for the Fe(CO)₃ subunit. Relative to Fe₂(S₂C₂H₄)(CO)₄(dppv), these bands are shifted to higher energy by about 50 cm⁻¹. A similar trend is observed for the propanedithiolato complexes.

The ³¹P NMR spectrum of [1(CO)₃]BF₄ shows two singlets in a 1:2 ratio, consistent with two isomers that differ with respect to the position of the dppv chelate.⁴ The smaller signal is assigned to a highly fluxional apical-basal isomer; this signal was found to broaden upon cooling the sample to -80 °C. A singlet assigned to the major isomer proved temperature-invariant, consistent with the dibasal stereochemistry. A similar trend is seen for [2(CO)₃]BF₄, except that the equilibrium concentration of the apical-basal isomer is barely detectable (Scheme 2, Table 1). The related Fe₂(S₂C₂H₄)(CO)₄(dppv) exhibits similar dynamics, although the apical-basal isomer is far more stabilized (20:1). In the -80 °C ³¹P NMR spectrum of [2(CO)₃]⁺, four isomers are observed, indicative of slowed folding of the propanedithiolate.

Substitution of [Fe₂(S₂C_nH_{2n})(CO)₃(dppv)(NO)]BF₄ by PMe₃. The salt [1(CO)₃]BF₄ proved highly reactive toward nucleophiles. Thus, treatment of [1(CO)₃]BF₄ with 1 equiv of PMe₃ at room temperature gave [1(CO)₂(PMe₃)]BF₄. The ³¹P NMR spectrum of [1(CO)₂(PMe₃)]BF₄ displayed singlets in both the dppv and PMe₃ regions, which implicates axial PMe₃ and dibasal dppv. The dibasal disposition of the dppv ligand is further evidenced by the ³¹P NMR chemical shift (δ74.1), following a pattern seen for related complexes.⁴

In a test of its relative electrophilicity, equimolar amounts of Fe₂(S₂C₂H₄)(CO)₄(dppv) and [1(CO)₃]BF₄ were treated with 1 equiv of PMe₃ at 20 °C. IR and ³¹P NMR measurements revealed exclusive consumption of [1(CO)₃]BF₄. In an attempt to elucidate some details of the substitution mechanism, a solution of [1(CO)₃]BF₄ was treated with 1 equiv of PMe₃ at -20 °C; we observed the complete disappearance of free PMe₃, partial consumption of [1(CO)₃]⁺, and the appearance of an intermediate species (ν_{NO} = 1727 cm⁻¹). This reaction appears to rapidly give the double adduct [1(CO)₃(PMe₃)₂]⁺, followed by a slower dissociation of PMe₃ that reacts with remaining starting materials (eqs 1 and 2).



Upon warming to room temperature, the mixture of [1(CO)₃]⁺ and the intermediate converted with good efficiency to [1(CO)₂(PMe₃)]⁺. When a solution of [1(CO)₃]⁺ was treated with excess PMe₃ at -20 °C, electrospray

- (6) Foster, M. W.; Cowan, J. A. *J. Am. Chem. Soc.* **1999**, *121*, 4093–4100. Stamler, J. S. S. D. J.; Loscalzo, J. *Science* **1992**, *258*, 1898–1902. Harrop, T. C.; Song, D.; Lippard, S. J. *J. Am. Chem. Soc.* **2006**, *128*, 3528–9. Huang, H.-W.; Tsou, C.-C.; Kuo, T.-S.; Liaw, W.-F. *Inorg. Chem.* **2008**, *47*, 2196–2204.
- (7) Krasna, A. I.; Rittenberg, D. *Proc. Nat. Acad. Sci.* **1954**, *40*, 225–227. Ahmed, A.; Lewis, R. S. *Biotechnol. Bioeng.* **2007**, *97*, 1080–1086.
- (8) Richter-Addo, G. B.; Legzdins, P. *Metal Nitrosyls*; Oxford University Press: New York, 1992.
- (9) Ezzaher, S.; Capon, J.-F.; Gloaguen, F.; Pétilon, F. Y.; Schollhammer, P.; Talarmin, J.; Pichon, R.; Kervarec, N. *Inorg. Chem.* **2007**, *46*, 3426–3428.
- (10) Treichel, P. M. C. R. A.; Matthews, R.; Bonnin, K. R.; Powell, D. J. *Organomet. Chem.* **1991**, *402*, 233–248. Georgakaki, I. P.; Miller, M. L.; Darensbourg, M. Y. *Inorg. Chem.* **2003**, *42*, 2489–2494.
- (11) Haines, R. J.; de Beer, J. A.; Greatrex, R. *J. Chem. Soc., Dalton Trans.* **1976**, 1749–1757.
- (12) Arabi, M. S.; Mathieu, R.; Poilblanc, R. *Inorg. Chim. Acta* **1977**, *23*, L17–L18.

- (13) Olsen, M. T.; Bruschi, M.; De Gioia, L.; Rauchfuss, T. B.; Wilson, S. R. *J. Am. Chem. Soc.* **2008**, *130*, 12021–12030.

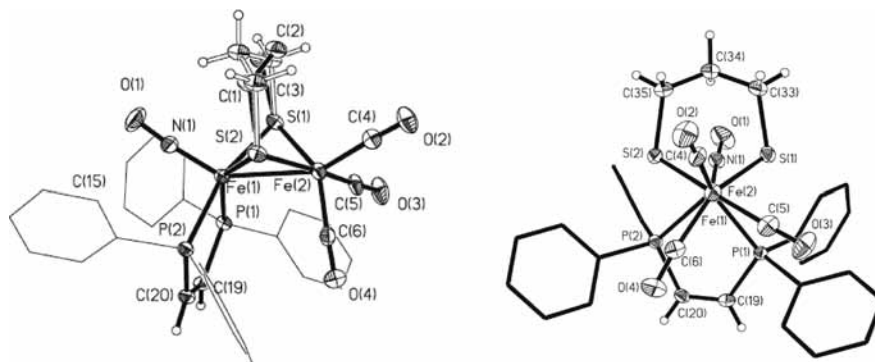


Figure 1. Side-on (left) and end-on (right) views of $[2(\text{CO})_3]\text{BF}_4$. Thermal ellipsoids are shown at 35% probability and are omitted on the phenyl rings for clarity, as are the anions (one phenyl group is perpendicular to the plane of the page). Selected bond distances (Å): Fe(1)–Fe(2), 2.5931(7); Fe(1)–P(1), 2.2791(10); Fe(1)–P(2), 2.3128(10); Fe(1)–N(1), 1.659(2); Fe(2)–C(4), 1.806(3); Fe(2)–C(5), 1.806(3); Fe(2)–C(6), 1.785(3).

Scheme 2. Isomerization Processes for the $\text{Fe}(\text{dppv})(\text{NO})^+$ Subunit

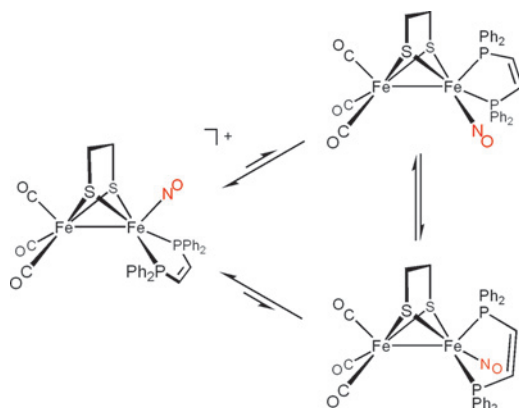


Table 1. Ratios of Apical-Basal/Dibasal Isomers (dppv Location) for $[\text{Fe}_2(\text{S}_2\text{C}_n\text{H}_{2n})(\text{CO})_{4-x}(\text{dppv})(\text{NO})_x]^{\text{t+}}$

$(\text{S}_2\text{C}_2\text{H}_4)(\text{CO})_4$	$(\text{S}_2\text{C}_2\text{H}_4)(\text{CO})_3(\text{NO})$	$(\text{S}_2\text{C}_3\text{H}_6)(\text{CO})_4$	$(\text{S}_2\text{C}_3\text{H}_6)(\text{CO})_3(\text{NO})$
20:1	1:2	7:1	1:>25(est.)

ionization mass spectrometry (ESI-MS) analysis of the reaction mixture confirmed the presence of a species corresponding to $[\mathbf{1}(\text{CO})_3(\text{PMe}_3)_2]^+$. The related reaction of $[2(\text{CO})_3]^+$ with PMe_3 gave similar results. The ^{31}P NMR spectrum of the intermediate in the PMe_3 region ($\sim\delta 25$) revealed one major and two minor isomers, and in each, the PMe_3 groups are nonequivalent, as virtually required since only low-symmetry products could be produced.

Solutions of $[2(\text{CO})_3(\text{PMe}_3)_2]\text{BF}_4$ readily produced crystals suitable for analysis by X-ray diffraction. The structure of $[2(\text{CO})_3(\text{PMe}_3)_2]^+$ features both octahedral and trigonal-bipyramidal iron centers, which are assigned as Fe(II) and Fe(0), respectively. The octahedral site features cis thiolates, cis phosphines, and cis carbonyl ligands. Viewing the pentacoordinate site as a trigonal bipyramid, the axial sites are occupied by the acceptor ligands, CO and NO^+ (Figure 2).

The crystallographic result shows that two molecules of PMe_3 added to the $\text{Fe}(\text{CO})_3$ site, inducing the migration of CO and scission of Fe–Fe and Fe–S bonds.

Cyano–Nitrosyl Complexes. The treatment of $[\mathbf{1}(\text{CO})_3]\text{BF}_4$ with 2 equiv of Et_4NCN gave the dicyanide, $\text{Et}_4\text{N}[\mathbf{1}(\text{CN})_2(\text{CO})]$. Shown in Figure 3, variable-temperature ^{31}P NMR measurements indicate that $\text{Et}_4\text{N}[\mathbf{1}(\text{CN})_2(\text{CO})]$ exists exclusively as a single diastereomer in solution wherein

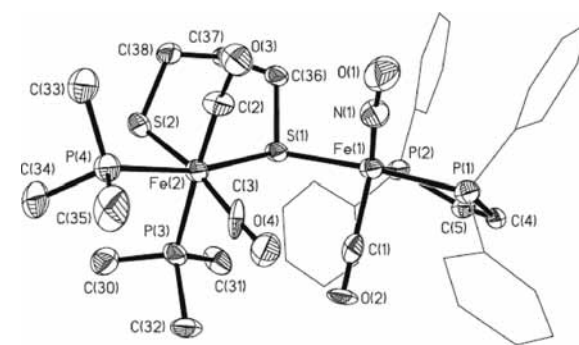


Figure 2. Structure of the cation in $[2(\text{CO})_3(\text{PMe}_3)_2]\text{BF}_4$. Thermal ellipsoids are shown at 35% probability and are omitted on the phenyl rings for clarity, as are the anions. Selected bond distances (Å): Fe(1)–N(1), 1.618(9); Fe(1)–C(1), 1.860(11); Fe(1)–P(1), 2.231(3); Fe(1)–P(2), 2.270(3); Fe(1)–S(1), 2.323(3); Fe(2)–S(1), 2.376(2); Fe(2)–S(2), 2.306(3); Fe(2)–C(2), 1.749(11); Fe(2)–C(3), 1.741(11); Fe(2)–P(3), 2.312(3); Fe(2)–P(4), 2.270(3); Fe(1)–Fe(2), 3.969.

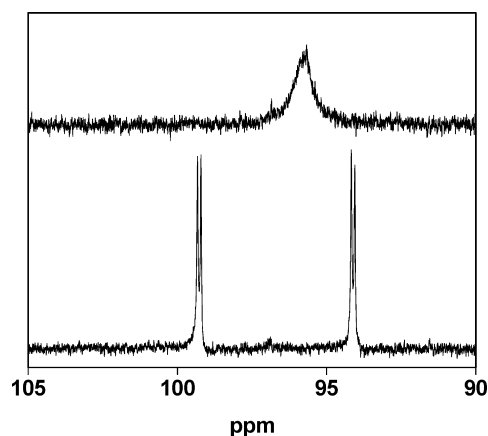


Figure 3. The 202 MHz ^{31}P NMR spectra of $\text{Et}_4\text{N}[\mathbf{1}(\text{CN})_2(\text{CO})]$ (CD_2Cl_2 soln) at 20 (top) and -60 °C (bottom).

the dppv is apical-basal. We propose that this reaction proceeds via relocation of the nitrosyl to the $\text{Fe}(\text{CN})_2$ site. The IR spectrum of $\text{Et}_4\text{N}[\mathbf{1}(\text{CN})_2(\text{CO})]$ resembles that for $[\mathbf{1}(\text{CO})(\text{dppv})]\text{BF}_4$ in the ν_{CO} region, but ν_{NO} occurs at 41 cm^{-1} lower energy. The switch of the dppv to apical-basal geometry is also consistent with a $\text{Fe}(\text{dppv})\text{CO}$ site; in $\text{Fe}(\text{dppv})\text{NO}$ sites, the dppv is invariably dibasal in the absence of extreme steric effects.

One equivalent of $[\mathbf{1}(\text{CO})_3]\text{BF}_4$ was found to rapidly consume 2 equiv of Et_4NCN . This behavior is analogous to the reaction of PMe_3 and $[\mathbf{1}(\text{CO})_3]\text{BF}_4$ (see above). When

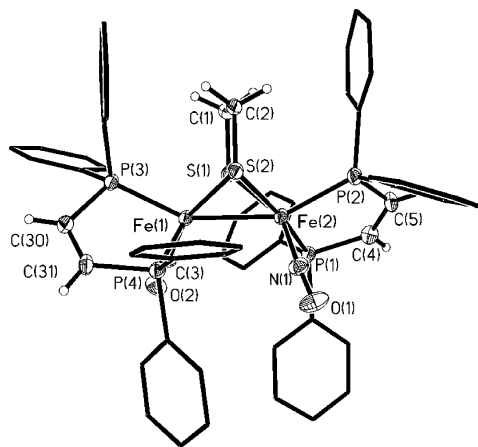


Figure 4. Structure of $[1(\text{CO})(\text{dppv})]$. Thermal ellipsoids are shown at 35% probability and are omitted on the phenyl rings for clarity. Selected bond distances (Å): Fe(1)–Fe(2), 2.5528(13); Fe(2)–P(1), 2.253(2); Fe(2)–P(2), 2.237(2); Fe(2)–N(1), 1.695(6); Fe(1)–C(3), 1.719(7); Fe(1)–P(3), 2.2026(19); Fe(1)–P(4), 2.247(2).

examined by IR spectroscopy at $-45\text{ }^{\circ}\text{C}$, the dicyanation of $[1(\text{CO})_3]\text{BF}_4$ generated a complex mixture characterized by several bands in the ν_{CO} and ν_{CN} regions, although the region $1800\text{--}1600\text{ cm}^{-1}$ was blank,¹³ implying the presence of a bridging NO ligand.

Despite their high electrophilicity, neither $[1(\text{CO})_3]\text{BF}_4$ nor $[2(\text{CO})_3]\text{BF}_4$ were observed to form adducts with CO, even at $-80\text{ }^{\circ}\text{C}$. This behavior contrasts with the monodentate bis(phosphine) nitrosyl complexes, $[\text{Fe}_2(\text{S}_2\text{C}_n\text{H}_{2n})(\text{CO})_3(\text{PMe}_3)_2(\text{NO})]\text{BF}_4$ ($n = 2, 3$), which reversibly bind CO. Thus, it is not surprising that $[1(\text{CO})_3]\text{BF}_4$ and $[2(\text{CO})_3]\text{BF}_4$ react with excess PMe_3 only near $-20\text{ }^{\circ}\text{C}$, whereas at comparable reactant concentrations, $[\text{Fe}_2(\text{S}_2\text{C}_n\text{H}_{2n})(\text{CO})_3(\text{PMe}_3)_2(\text{NO})]\text{BF}_4$ react immediately with PMe_3 at $-80\text{ }^{\circ}\text{C}$.

NO As a Trapping Agent for Mixed-Valence Species: $[\text{Fe}_2(\text{S}_2\text{C}_2\text{H}_4)(\text{CO})_2(\text{dppv})_2(\text{NO})]^+$ and Related Species. Treatment of $[1(\text{CO})_3]\text{BF}_4$ with 1 equiv of dppv slowly and inefficiently afforded the bis(diphosphine), $[1(\text{CO})(\text{dppv})_2]\text{BF}_4$. Alternatively, $[1(\text{CO})(\text{dppv})]\text{BF}_4$ also arises in the reaction of the dicarbonyl¹⁴ $\text{Fe}_2(\text{S}_2\text{C}_2\text{H}_4)(\text{CO})_2(\text{dppv})_2$ with NOBF_4 . This route suffered from the tendency of the mononitrosyl to further react with NOBF_4 to irreversibly yield, inter alia, $\text{Fe}(\text{dppv})(\text{NO})_2$. A potentially versatile route to diiron nitrosyl complexes entails a two-step process that involves one-electron oxidation of diiron(I) precursors followed by treatment with NO. Oxidation of $\text{Fe}_2(\text{S}_2\text{C}_2\text{H}_4)(\text{CO})_2(\text{dppv})_2$ ¹⁴ and trapping with NO gave the corresponding mononitrosyl $[\text{Fe}_2(\text{S}_2\text{C}_2\text{H}_4)(\text{NO})(\text{CO})(\text{dppv})_2]\text{BF}_4$ ($[1(\text{dppv})(\text{CO})]\text{BF}_4$). The ^{31}P NMR spectrum of $[1(\text{dppv})(\text{CO})]\text{BF}_4$ showed four broad singlets at $25\text{ }^{\circ}\text{C}$, which sharpened upon cooling the sample to $-80\text{ }^{\circ}\text{C}$. We conclude that the two dppv ligands span apical-basal coordination sites, as observed crystallographically in the solid state (Figure 4), but that the dynamic racemization process is subject to a low activation barrier. The precursor complex also exhibits a related dynamic process, but at a higher barrier.¹⁴ The complex

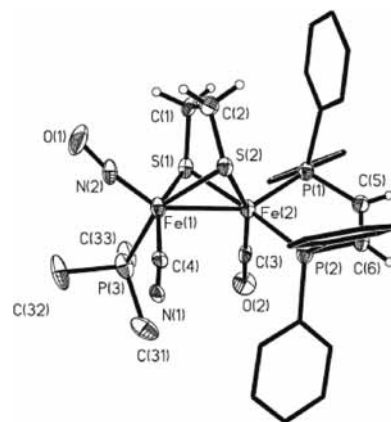
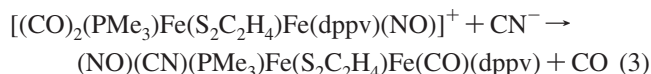


Figure 5. Structure of $1(\text{CN})(\text{CO})(\text{PMe}_3)$. Thermal ellipsoids are shown at 35% probability and are omitted on the phenyl rings for clarity. Distances (Å): Fe(1)–Fe(2), 2.275(4); Fe(1)–N(2), 1.631(12); Fe(1)–P(3), 2.275(4); Fe(1)–C(4), 1.926(15); Fe(2)–P(1), 2.183(4); Fe(2)–P(2), 2.208(4); Fe(2)–C(3), 1.713(14).

$[1(\text{dppv})(\text{CO})]\text{BF}_4$ is the only diiron dithiolate nitrosyl observed in this series that features a basal nitrosyl ligand present in the major observed isomer. ^{31}P NMR studies at low temperatures showed that $[1(\text{CO})(\text{dppv})]\text{BF}_4$ binds CO reversibly (see Supporting Information).

Oxidation of $\text{Fe}_2(\text{S}_2\text{C}_3\text{H}_6)(\text{CO})_4(\text{dppv})$ with 1 equiv of FcBF_4 followed by the addition of about 1 equiv of NO gave $[2(\text{CO})_3]\text{BF}_4$. We also prepared $[1(\text{CO})_2(\text{PMe}_3)]\text{BF}_4$ via the mixed valence species $[\text{Fe}_2(\text{S}_2\text{C}_2\text{H}_4)(\text{CO})_3(\text{dppv})(\text{PMe}_3)]\text{BF}_4$.⁴

Nitrosyl Migrations: $\text{Fe}_2(\text{S}_2\text{C}_2\text{H}_4)(\text{CN})(\text{CO})(\text{dppv})(\text{PMe}_3)(\text{NO})$. Whereas $\text{Fe}_2(\text{S}_2\text{C}_2\text{H}_4)(\text{CO})_3(\text{dppv})(\text{PMe}_3)$ is inert toward substitution by cyanide, its nitrosylated derivative $[1(\text{CO})_2(\text{PMe}_3)]\text{BF}_4$ was found to react with 1 equiv of cyanide to produce $1(\text{CN})(\text{CO})(\text{PMe}_3)$. The ^{31}P NMR spectrum of $1(\text{CN})(\text{CO})(\text{PMe}_3)$ consisted of two doublets in the dppv region, indicative of a single diastereomer. Apparently, rapid turnstile rotation^{4,14} equilibrates the diastereomeric rotamers. The structure of this species was confirmed crystallographically; the compound is chiral and crystallizes as the racemate (Figure 5). Carbonyl, cyanide, and nitrosyl ligands were distinguished by their bond lengths; the crystallographic refinement also clearly favored one set of assignments. The dppv spans the apical-basal sites, as is typical for $\text{Fe}(\text{CO})(\text{dppv})$ centers.⁴ Cyanide and PMe_3 are basal and NO is apical, as is typical in this series of compounds. Distinctively, the nitrosyl is no longer bound to the same Fe as the dppv, a finding that implicates the intramolecular migration of NO (eq 3).



A similar NO migration reaction had been implicated for the cyanation of $[\text{Fe}_2(\text{S}_2\text{C}_3\text{H}_6)(\text{CO})_4(\text{PMe}_3)(\text{NO})]\text{BF}_4$, which gives $\text{Fe}_2(\text{S}_2\text{C}_3\text{H}_6)(\text{CN})(\text{CO})_3(\text{PMe}_3)(\text{NO})$.¹³

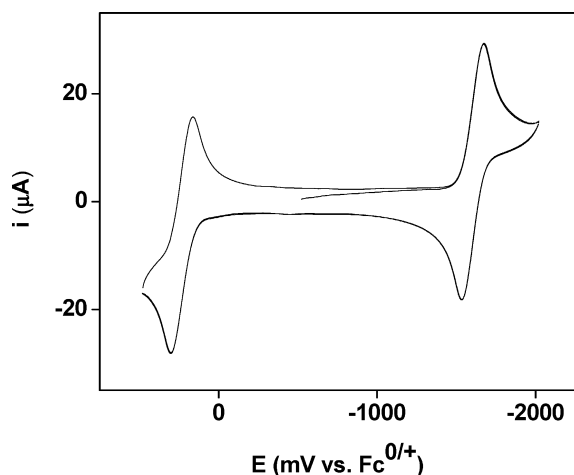
IR data for the compounds discussed in this work are given in Table 2.

Electrochemistry of Nitrosyl Derivatives. Cyclic voltammetric studies showed that replacement of CO by NO^+ shifts the first reduction and first oxidation events by ca. 1 V anodically, an effect that is akin to that of protonation

(14) Justice, A. K.; Zampella, G.; De Gioia, L.; Rauchfuss, T. B. *Chem. Commun.* **2007**, 2019–21.

Table 2. IR Data (cm⁻¹, CH₂Cl₂ soln) for Selected Compounds

compound	ν_{CO}	ν_{NO}
[1(CO) ₃] ⁺	2070, 2006	1796
[1(CO) ₂ (PMe ₃) ⁺	2002, 1958	1775
[1(CO)(dppv)] ⁺	1928	1760
1(CO)(PMe ₃)(CN)	1910	1734
[1(CN) ₂ (CO)] ⁻	1923	1719

**Figure 6.** Cyclic voltammogram of 1 mM [1(CO)(dppv)]BF₄ in CH₂Cl₂ solution (50 mM Bu₄NPF₆, 20 °C, 100 mV/s).**Table 3.** Redox Properties for Selected Nitrosyl Complexes^a

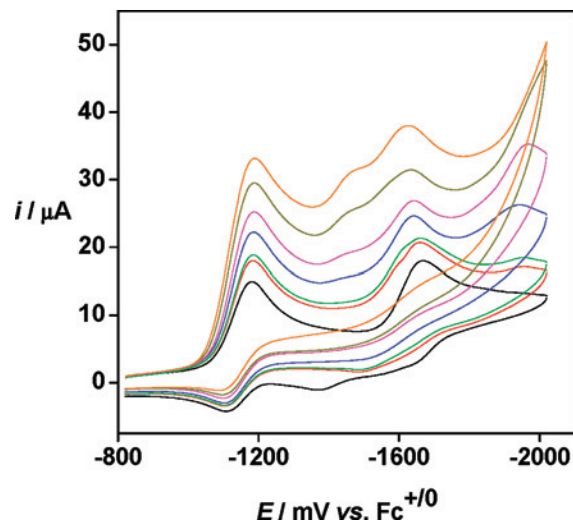
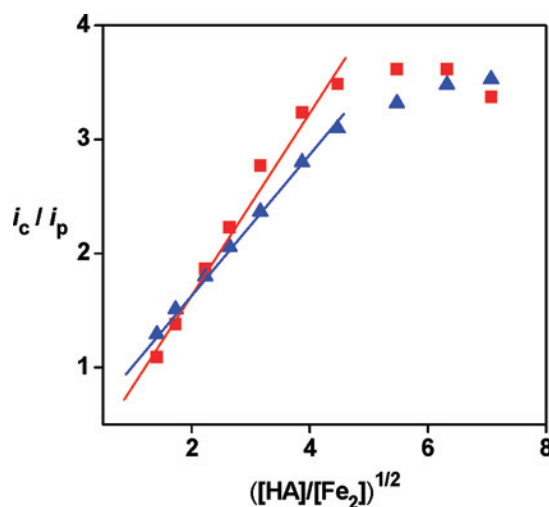
compound	oxidation (V)	reduction (V)
Fe ₂ (S ₂ C ₂ H ₄)(CO) ₄ (dppv)	-0.06	-2.07 ^b
[1(CO) ₃] ⁺	> 1	-1.15 ^d , -1.61 ^d
[2(CO) ₃] ⁺	> 1	-1.21 ^d , -1.73 ^d
Fe ₂ (S ₂ C ₂ H ₄)(CO) ₃ (dppv)(PMe ₃) ⁴	-0.300 ^b	
[1(CO) ₂ (PMe ₃) ⁺	0.850	-1.51 ^c , -1.99 ^b
Fe ₂ (S ₂ C ₂ H ₄)(CO) ₂ (dppv) ₂	-0.695 ^c	
[1(CO)(dppv)] ⁺	0.22 ^c	-1.62 ^c

^a Potentials are referenced against Ag/AgCl. Voltammograms recorded in CH₂Cl₂ solution with 50 mM Et₄NPF₆, at 100 mV/s. ^b Irreversible. ^c Reversible. ^d Reversible at scan rates <100 mV/s.

(Figure 6). Furthermore, the observed redox events are typically reversible: the species, [1(CO)₃]⁺, reduces quasi-reversibly at -630 and -1.090 mV versus Ag/AgCl. The bulky complex [1(CO)(dppv)]⁺ can be reversibly oxidized and reduced (see Table 3).

Given their mild reduction potentials, we assayed the redox properties of the diiron nitrosyl complexes in the presence of acids. The simple dppv complexes [1(CO)₃]BF₄ and [2(CO)₃]BF₄ exhibited catalytic waves at their primary reductions, both of which were mild (-1.15 and -1.21 V, respectively, versus the Fc^{0/+} couple, see Figure 7).

At the concentration ratio of [CF₃CO₂H]/([2(CO)₃]⁺) ≤ 20, no catalysis was observed at the potential of the second reduction step. This behavior is explicable if the acid in the diffusion layer is consumed during the first reduction wave. A rough estimate of the catalytic efficiency of the FeNO derivatives can be obtained from the variation of the catalytic peak current with the acid concentration. As shown in Figure 8, the peak current varies linearly with the square root of the acid concentration, which indicates that the rate-determining step in the catalytic reaction is first-order in acid

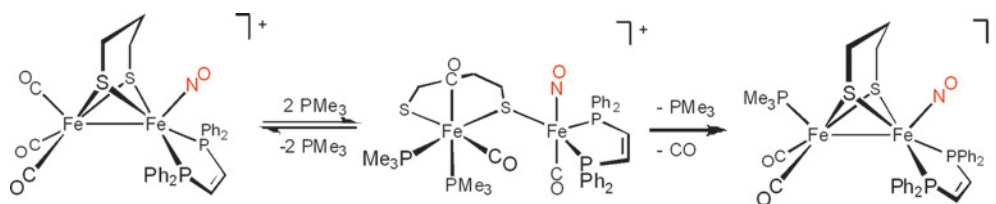
**Figure 7.** Cyclic voltammograms of complex [2(CO)₃]BF₄ in a 1 mM CH₂Cl₂ (~50 mM Bu₄NPF₆) solution as a function of [CF₃CO₂H] (0, 1, 2, 3, 5, 7, and 10 expressed as molar equiv). Scan rate 100 mV s⁻¹ at a glassy carbon electrode 0.3 cm in diameter.**Figure 8.** Plots of the catalytic current as a function of the acid concentration for [1(CO)₃]⁺ (squares) and [2(CO)₃]⁺ (triangles): i_c and i_p are the peak currents in the presence and in the absence of acid, respectively.

(see the Supporting Information).¹⁵ We estimated (see the Experimental Section) an overall catalytic rate constant $k' \sim 130$ and $100 \text{ M}^{-1} \text{ s}^{-1}$ for [1(CO)₃]⁺ and [2(CO)₃]⁺, respectively. These values compare well with those calculated by the same procedure for cobaloxime catalysts, which are known to be highly efficient.¹⁶ Note however that the overall rate constant k' does not reflect precisely the rate-determining step but is a composite of equilibrium and rate constants.

At high [H⁺], the catalytic current becomes almost independent of the acid concentration, indicative of a change in the rate-determining step, which could be the release of H₂, as has

(15) Bard, A. J.; Faulkner, L. R. *Electrochemical Methods Fundamentals and Applications*; J. Wiley: New York, 2001.

(16) Hu, X. L.; Brunschwig, B. S.; Peters, J. C. *J. Am. Chem. Soc.* **2007**, *129*, 8988–8998.

Scheme 3. Pathway Proposed for Substitution of $[2(\text{CO})_3]^+$ by PMe_3 

been proposed previously.¹⁶ Catalysis by $[\mathbf{1}(\text{CO})_3]^+$ and $[2(\text{CO})_3]^+$ is unaffected by the presence of CO, although the corresponding hexacarbonylcatalysts are poisoned by CO.¹⁷

Compounds $[\mathbf{1}(\text{CO})_3]^+$ and $[2(\text{CO})_3]^+$ are not protonated even in the presence of excess triflic acid, consistent with proton reduction catalysis that is initiated by electron-transfer (E step) followed by protonation (C step). The sequence of the two subsequent steps, EC or CE, is unknown. Consistent with the EC mechanism, $[\mathbf{1}(\text{CO})(\text{dppv})]\text{BF}_4$ was chemically reduced with ~ 1.1 equiv of decamethylcobaltocene at -78 °C to generate the radical $\mathbf{1}(\text{CO})(\text{dppv})$. The IR spectrum indicated that reduction is localized on FeNO : ν_{CO} shifted from 1918 to 1886 cm^{-1} , but ν_{NO} shifted by nearly 180 cm^{-1} from 1748 to 1571 cm^{-1} . Upon exposure of these solutions to air, the signals for $[\mathbf{1}(\text{CO})(\text{dppv})]^+$ were restored. X-band EPR spectrum of the frozen reduced solution revealed a slightly rhombic signal ($g = 1.95350, 1.98051, 2.01355$), where the low field signal exhibits a large 60 MHz splitting, consistent with ^{14}N hyperfine coupling.

Discussion

Nitrosylation provides an easy means to significantly modify the electronic environment of the diiron dithiolate carbonyls without altering its formal oxidation state. Replacement of CO by NO^+ causes ν_{CO} to increase by 50 cm^{-1} (Table 1). Such shifts in ν_{CO} are about half the effect induced by protonation of related diiron complexes.¹⁸ The nitrosyl derivatives exhibit an enhanced tendency to undergo substitution reactions as well as to serve as proton reduction catalysts at potentials approaching the thermodynamic limit.¹⁹ The EPR spectrum of $\text{Fe}_2(\text{S}_2\text{C}_2\text{H}_4)(\text{CO})(\text{N})(\text{dppv})_2$ indicates that reduction is localized on the FeNO subunit.

As shown in this and the previous report, NO^+ induces novel stereochemistry on the diiron site. In contrast to all other ligands evaluated on diiron(I) dithiolates, NO^+ displays a high preference for the apical site. The complexes characterized in this work all exhibit apical NO^+ ligands, except for the $(\text{dppv})_2$ derivatives where steric factors destabilize the isomer containing with both dibasal and apical-basal diphosphines. Even this complex is less stereochemically rigid than the analogous carbonyl derivative.

The structure and reactivity of the complexes $[\text{Fe}_2(\text{S}_2\text{C}_3\text{H}_6)(\text{CO})_3(\text{PR}_3)_2(\text{NO})]^+$ strongly depends on whether

the two phosphines are dppv or PMe_3 . The complex $[\text{Fe}_2(\text{S}_2\text{C}_3\text{H}_6)(\text{CO})_3(\text{PMe}_3)_2(\text{NO})]^+$ adopts a strongly distorted “rotated” structure,¹³ whereas $[\mathbf{1}(\text{CO})_3]^+$ adopts the normal distorted- C_{2v} motif. We suggest that the electronic asymmetry of the $(\text{PMe}_3)_2$ derivatives, which feature $\text{Fe}(\text{CO})_2(\text{PMe}_3)$ and $\text{Fe}(\text{NO})(\text{CO})(\text{PMe}_3)^+$ sites, is greater than for the dppv derivatives described in this work.

The new nitrosyl diiron(I) complexes were prepared by three methods:

(1) *Direct Electrophilic Nitrosylation by Attack of NO^+* . This method is effective but limited by the range of substituted diiron dithiolates, since the diiron center must contain some donor ligands; the hexacarbonyls do not form isolable derivatives upon reaction with NOBF_4 . We propose that the electrophilic nitrosylation proceeds similarly to the protonation of diiron complexes, that is, by attack of the electrophile at a terminal metal site.⁹ We have shown that related $36e^-$ diiron nitrosyl complexes are prone to decarbonylation.¹³

(2) *Nitrosylation by Attack of NO on Mixed Valence Diiron Complexes*. This method is complementary to the previous one. It has been shown that NO^+ reacts with some metal carbonyls via inner-sphere electron transfer followed by dissociation of NO .²⁰ Many of the oxidized diiron carbonyl dithiolates studied by us previously react with NO .

(3) *Substitution of Diiron Nitrosyl Complexes*. The considerable electrophilicity of $[\mathbf{1}(\text{CO})_3]\text{BF}_4$ is indicated both by the rate and the stoichiometry of its substitution reactions. The presence of the nitrosyl allows the preparation of highly substituted diiron(I) complexes, which would be difficult to prepare without NO^+ . These include $[\text{Fe}_2(\text{S}_2\text{C}_2\text{H}_4)(\text{CN})_2(\text{CO})(\text{dppv})(\text{NO})]^-$ and the chiral-at-metal derivative $\text{Fe}_2(\text{S}_2\text{C}_2\text{H}_4)(\text{CN})(\text{PMe}_3)(\text{CO})(\text{dppv})(\text{NO})$. The facility of the intermetallic migration of NO^+ limits the range of isolable substituted products. Also impressive is the rate of substitutions: the cyanations of $\text{Fe}_2(\text{S}_2\text{C}_3\text{H}_6)(\text{CO})_6$ at 25 °C and $[2(\text{CO})_3]\text{BF}_4$ at -78 °C were found to proceed at comparable rates. This temperature difference roughly corresponds to a 30% decrease in activation energy.

One striking finding is the tendency of $[\text{Fe}_2(\text{S}_2\text{C}_n\text{H}_{2n})(\text{CO})_3(\text{dppv})(\text{NO})]^+$ to undergo substitution via the intermediacy of a 2:1 adduct, as illustrated by $[(\text{PMe}_3)_2(\text{CO})_2\text{Fe}(\text{S}_2\text{C}_n\text{H}_{2n})\text{Fe}(\text{CO})(\text{dppv})(\text{NO})]^+$ (Scheme 3). These adducts form via the scission of the $\text{Fe}-\text{Fe}$ bond and one $\text{Fe}-\text{S}$ bond. The 2:1 adducts illustrate the possibility that other $[\text{Fe}(\text{I})_2]$ species substitute via mixed-valence adducts. Such a mechanism may be relevant to the finding that attempted monocyanoation of

(17) Borg, S. J.; Behrsing, T.; Best, S. P.; Razavet, M.; Liu, X.; Pickett, C. J. *J. Am. Chem. Soc.* **2004**, *126*, 16988–16999.

(18) Zhao, X.; Hsiao, Y.-M.; Lai, C.-H.; Reibenspies, J. H.; Darensbourg, M. Y. *Inorg. Chem.* **2002**, *41*, 6573–6582. (a) Gloaguen, F.; Lawrence, J. D.; Rauchfuss, T. B.; Bénard, M.; Rohmer, M.-M. *Inorg. Chem.* **2002**, *41*, 6573–6582.

(19) Felton, G. A. N.; Glass, R. S.; Lichtenberger, D. L.; Evans, D. H. *Inorg. Chem.* **2006**, *45*, 9181–9184.

(20) Connelly, N. G.; Demidowicz, Z.; Kelly, R. L. *Dalton Trans.* **1975**, 2335–2340. Ashford, P. K.; Baker, P. K.; Connelly, N. G.; Kelly, R. L.; Woodley, V. A. *J. Chem. Soc., Dalton Trans.* **1982**, 477–479.

Table 4. Details of Data Collection and Structure Refinement

	[2(CO) ₃]BF ₄	[1(CO) ₂ (PMe ₃)]BF ₄
chemical formula	C ₃₂ H ₂₈ BF ₄ Fe ₂ NO ₄ P ₂ S ₂	C ₃₅ H ₃₉ BCl ₄ F ₄ Fe ₂ NO ₃ P ₃ S ₂
fw	815.12	1019.01
<i>T</i> (K)	193(2)	193(2)
space group	<i>P</i> 2 ₁ / <i>c</i>	<i>P</i> 2 ₁ / <i>n</i>
<i>a</i> (Å)	10.094(4)	15.2650(11)
<i>b</i> (Å)	17.701(7)	19.3588(13)
<i>c</i> (Å)	19.493(8)	15.5567(11)
α (deg)	90	90
β (deg)	97.814(6)	95.573(3)
γ (deg)	90	90
<i>Z</i>	4	4
<i>V</i> (Å ³)	3451(2)	4575.5(6)
λ (Å)	0.71073	0.71073
<i>D</i> _{calcd} (g cm ⁻³)	0.001569	0.001479
μ (cm ⁻¹)	0.01114	0.01114
<i>R</i> (<i>F</i> _o ²)	0.0278	0.0406
<i>R</i> _w (<i>F</i> _o ²)	0.0568	0.1086

	[1(CO)(dppv)]BF ₄	[1(CN)(CO)(PMe ₃)]BF ₄	[1(CO) ₃ (PMe ₃) ₂]BF ₄
chemical formula	C ₅₈ H ₅₄ BCl ₆ F ₄ Fe ₂ NO ₂ P ₄ S ₂	C ₃₃ H ₃₅ Fe ₂ N ₂ O ₂ P ₃ S ₂	C ₃₈ H ₄₆ BF ₄ Fe ₂ NO ₄ P ₄ S ₂
fw	1396.23	760.36	967.27
<i>T</i>	193(2)	193(2)	193(2)
space group	<i>P</i> 2 ₁	<i>Pna</i> 2 ₁	<i>P</i> 1
<i>a</i> (Å)	10.8808(16)	19.629(5)	13.4269(19)
<i>b</i> (Å)	17.757(3)	11.016(3)	13.637(2)
<i>c</i> (Å)	16.692(2)	32.186(9)	14.435(2)
α (deg)	90	90	74.158(9)
β (deg)	104.511(3)	90	73.229(9)
γ (deg)	90	90	79.917(9)
<i>Z</i>	2	8	2
<i>V</i> (Å ³)	3122.3(8)	6959(3)	2421.2(6)
λ (Å)	0.71073	0.71073	0.71073
<i>D</i> _{calcd} (g cm ⁻³)	0.001485	0.001451	0.001327
μ (cm ⁻¹)	0.00945	0.01124	0.00868
<i>R</i> (<i>I</i> > 2σ) ^a	0.0610	0.0886	0.0773
<i>R</i> _w (<i>I</i> > 2σ) ^b	0.1256	0.1186	0.1628

$$^a R = \sum |F_o| - |F_c| / \sum |F_o|. \quad ^b R_w = \{ [w(|F_o| - |F_c|)^2] / \sum [wF_o^2] \}^{1/2}, \text{ where } w = 1/\sigma^2(F_o).$$

Fe₂(S₂C₃H₆)(CO)₆ mainly affords the dicyanide.²¹ The presence of the NO ligand, a very strong acceptor, favors such electron-transfer processes. Related Fe–S scission reactions occur upon the reduction of diiron dithiolates.^{17,22}

Experimental Section

Methods have been recently described.²³ NOBF₄ was purified by rapid sublimation at 220 °C at ~0.01 mmHg and was stored in a dry glovebox at –30 °C. Since NOBF₄ is poorly soluble, the solid was ground to a fine powder prior to use in sensitive reactions.

Electrochemistry. Cyclic voltammetry experiments were conducted in a ~10-mL one-compartment glass cell, with a Pt wire (counter electrode) and a glassy carbon working electrode. All voltammograms were referenced versus a Ag/AgCl reference electrode (50 mM KCl).

[Fe₂(S₂C₂H₄)(CO)₃(dppv)(NO)]BF₄, [1(CO)₃]BF₄. A slurry of 0.141 g (1.21 mmol) of pulverized NOBF₄ in 20 mL of CH₂Cl₂ was treated with a solution of 0.865 g (1.21 mmol) of Fe₂(S₂C₂H₄)(CO)₄(dppv) in 100 mL of CH₂Cl₂. The reaction mixture was immediately cooled to 0 °C, and after 10 h, the deep

red reaction mixture was concentrated in vacuo. The addition of 50 mL of hexanes to the concentrated solution precipitated the dark-red-colored product. Yield: 0.912 g (94%). 500 MHz ¹H NMR (CD₂Cl₂): δ 8.6–7.2 (m, 20H, C₆H₅), 3.0 (dd, 2H, *PCH*), 2.05 (m, 1H, *SCH*), 1.6 (m, 1H, *SCH*), 1.3 (m, 1H, *SCH*), 0.8 (m, 1H, *SCH*). 202 MHz ³¹P NMR (CD₂Cl₂, 20 °C): δ 77.1 (s, dppv), 72.0 (s, dppv). ³¹P NMR (CD₂Cl₂, –80 °C): δ 78.5 (s, dppv), 73.3 (s, dppv). IR (CH₂Cl₂): ν_{CO} = 2070, 2006; ν_{NO} = 1796 cm⁻¹. ESI-MS: *m/z* 714.1 ([Fe₂(S₂C₂H₄)(CO)₃(dppv)(NO)]⁺). Anal. calcd (found) for C₃₁H₂₆BF₄Fe₂NO₄P₂S₂: C, 46.86 (46.86); H, 3.25 (3.27); N, 1.60 (1.75).

[Fe₂(S₂C₃H₆)(CO)₃(dppv)(NO)]BF₄, [2(CO)₃]BF₄. This compound was prepared following the method described for [1(CO)₃]BF₄. Yield: 2.0 g (88%). 500 MHz ¹H NMR (CD₂Cl₂, 20 °C): δ 8.5–8.2 (m, 20H, C₆H₅), 2.9 (bs, 2H, *PCH*), 2.6 (m, 4H, (SCH₂)₂CH₂), 2.0 (m, 2H, (SCH₂)₂CH₂). 202 MHz ³¹P NMR (CD₂Cl₂, 20 °C): δ 69.7 (s, dppv). ³¹P NMR (CD₂Cl₂, –80 °C): δ 76.7 (s, dppv), 75.1 (s, dppv), 72.4 (s, dppv), 69.5 (s, dppv). IR (CH₂Cl₂): ν_{CO} = 2069, 2005; ν_{NO} = 1788 cm⁻¹. ESI-MS: *m/z* 728.1 ([Fe₂(S₂C₃H₆)(CO)₃(dppv)(NO)]⁺). Anal. calcd (found) for C₃₁H₂₆BF₄Fe₂NO₄P₂S₂: C, 47.15 (46.56); H, 3.46 (3.41); N, 1.72 (1.86).

[Fe₂(S₂C₂H₄)(CO)₂(NO)(PMe₃)(dppv)]BF₄, [1(CO)₂(PMe₃)]BF₄. To a mixture of 0.200 g (0.263 mmol) of Fe₂(S₂C₂H₄)(CO)₃(dppv)(PMe₃)⁴ and 0.030 g (0.263 mmol) of finely pulverized NOBF₄ was added 15 mL of CH₂Cl₂. After stirring for 5 min, the solution was concentrated to 5 mL, and the dark red product was precipitated upon addition of 30 mL of hexanes. Crystals were

- (21) Gloaguen, F.; Lawrence, J. D.; Schmidt, M.; Wilson, S. R.; Rauchfuss, T. B. *J. Am. Chem. Soc.* **2001**, *123*, 12518–12527.
 (22) Felton, G. A. N.; Vannucci, A. K.; Chen, J.; Lockett, L. T.; Okumura, N.; Petro, B. J.; Zakai, U. I.; Evans, D. H.; Glass, R. S.; Lichtenberger, D. L. *J. Am. Chem. Soc.* **2007**, *129*, 12521–12530. (a) Aguirre de Carcer, I.; DiPasquale, A.; Rheingold, A. L.; Heinekey, D. M. *Inorg. Chem.* **2006**, *45*, 8000–8002.
 (23) Justice, A. K.; Nilges, M.; Rauchfuss, T. B.; Wilson, S. R.; De Gioia, L.; Zampella, G. *J. Am. Chem. Soc.* **2008**, *130*, 5293–5301.

grown via slow diffusion of hexanes into a CH_2Cl_2 solution of the complex. Yield: 0.19 g (86%). ^{31}P NMR (CD_2Cl_2 , 20 °C): δ 74.1 (s, dppv), 25.0 (s, PMe_3). ^{31}P NMR (CD_2Cl_2 , -70 °C): δ 78.1 (s, dppv), 75.7 (s, dppv), 26.8 (s, PMe_3), 23.0 (s, PMe_3). IR (CH_2Cl_2): $\nu_{\text{CO}} = 2002, 1958, \nu_{\text{NO}} = 1775$. In situ spectra (ReactIR 4000, Mettler-Toledo) indicated the presence of $[\text{Fe}_2(\text{S}_2\text{C}_2\text{H}_4)(\text{CO})_3(\text{dppv})(\text{PMe}_3)(\text{NO})]\text{BF}_4$ after 3 h of vigorous stirring at -78 °C: (CH_2Cl_2): $\nu_{\text{CO}} = 2037, 1992, 1957; \nu_{\text{NO}} = 1775$. ESI-MS: m/z 762.2 ($[\text{Fe}_2(\text{S}_2\text{C}_2\text{H}_4)(\text{CO})(\text{dppv})(\text{PMe}_3)(\text{NO})]^+$). Anal. calcd (found) for $\text{C}_{33}\text{H}_{35}\text{BF}_4\text{Fe}_2\text{NO}_3\text{P}_3\text{S}_2$: C, 46.67 (46.66); H, 4.15 (4.37); N, 1.65 (1.62).

Synthesis via Oxidation and Trapping with NO. To a solution of 0.196 g (0.258 mmol) of $\text{Fe}_2(\text{S}_2\text{C}_2\text{H}_4)(\text{CO})_3(\text{dppv})(\text{PMe}_3)^4$ in 15 mL of CH_2Cl_2 , cooled to -45 °C, was added 0.070 g (0.256 mmol) of FcBF_4 . The IR spectrum of the purple solution displayed signals matching $[\text{Fe}_2(\text{S}_2\text{C}_2\text{H}_4)(\text{CO})_3(\text{dppv})(\text{PMe}_3)]\text{BF}_4$.⁴ The reaction vessel was sealed and to the cooled solution was injected 6 mL (0.268 mmol) of NO gas. After 1 h, the IR spectrum of the resulting deep red solution matched that for $[\text{I}(\text{CO})_2(\text{PMe}_3)]\text{BF}_4$. The product precipitated upon the addition of 60 mL of hexanes. Yield: 0.116 g (53%). Analogous procedures were followed for the sequential oxidation and trapping of $\text{Fe}_2(\text{S}_2\text{C}_3\text{H}_6)(\text{CO})_4(\text{dppv})$ to give $[\text{Fe}_2(\text{S}_2\text{C}_3\text{H}_6)(\text{CO})_3(\text{dppv})(\text{NO})]\text{BF}_4$: To a solution of 0.045 g (0.062 mmol) of $\text{Fe}_2\text{S}_2\text{C}_3\text{H}_6$ in 5 mL of CH_2Cl_2 , cooled to -45 °C, was added a solution of 0.017 g (0.062 mmol) of FcBF_4 in 5 mL of CH_2Cl_2 . To the resultant reaction mixture was added 3.2 mL of NO (0.124 mmol), and the reaction vessel was sealed. After 20 min, the IR spectrum matched that of $[\text{2}(\text{CO})_3]\text{BF}_4$, and the product was precipitated upon the addition of 50 mL of hexanes. Yield: 77%.

$[\text{Fe}_2(\text{S}_2\text{C}_2\text{H}_4)(\text{CO})(\text{dppv})_2(\text{NO})]\text{BF}_4$, $[\text{I}(\text{CO})(\text{dppv})]\text{BF}_4$. To a solution of 0.150 g (0.142 mmol) of $\text{Fe}_2(\text{S}_2\text{C}_2\text{H}_4)(\text{CO})_2(\text{dppv})_2$ in 20 mL of CH_2Cl_2 , cooled to -45 °C, was added 0.039 g (0.142 mmol) of FcBF_4 . An immediate IR spectrum of the dark brown solution displayed signals attributed to $[\text{Fe}_2(\text{S}_2\text{C}_2\text{H}_4)(\text{CO})(\mu\text{-CO})(\text{dppv})_2]\text{BF}_4$: $\nu_{\text{CO}} = 1959$ (s), 1887 (w, br) cm^{-1} .²³ The reaction vessel was sealed, and to the cooled solution was injected 3.6 mL (0.161 mmol) of NO gas. After 1 h, the resultant dark brown solution displayed an IR spectrum corresponding to $[\text{I}(\text{CO})(\text{dppv})]\text{BF}_4$. The solution was warmed to room temperature and concentrated in vacuo to ~5 mL. The product precipitated upon the addition of 30 mL of Et_2O . Impurities observed in the ^{31}P NMR spectrum can be removed after several recrystallizations from $\text{CH}_2\text{Cl}_2\text{-Et}_2\text{O}$. Yield: 0.080 g (49%). ^1H NMR (CD_2Cl_2): δ 8.2–6.8 (m, 40H, dppv), 1.7–0.8 (m, 4 H, $\text{SCH}_2\text{CH}_2\text{S}$). ^{31}P NMR (CD_2Cl_2 , 20 °C): δ 101.7 (br s, dppv), 87.8 (broad s, dppv), 81.2 (br s, dppv), 74.9 (br s, dppv). IR (CH_2Cl_2): $\nu_{\text{CO}} = 1928, \nu_{\text{NO}} = 1760 \text{ cm}^{-1}$. ESI-MS: m/z 1054.2 ($[\text{Fe}_2(\text{S}_2\text{C}_2\text{H}_4)(\text{CO})(\text{dppv})_2(\text{NO})]^+$). Acceptable CHN analyses were not obtainable. Anal. calcd (found) for $\text{C}_{55}\text{H}_{48}\text{BF}_4\text{Fe}_2\text{NO}_2\text{P}_4\text{S}_2$: C, 57.87 (56.00); H, 4.24 (4.00); N, 1.23 (1.31). An excess of NOBF_4 gave $\text{Fe}(\text{dppv})(\text{NO})_2$:²⁴ $\nu_{\text{NO}} = 1718$ and 1666 cm^{-1} ; ESI-MS: m/z 512.

Alternative routes were examined: the addition of dppv to $[\text{I}(\text{CO})_3]$ and the treatment of $\text{Fe}_2(\text{S}_2\text{C}_2\text{H}_4)(\text{CO})_2(\text{dppv})_2$ with NOBF_4 . The raw product contained the targeted complex as well as unidentified impurities, as indicated by the ^{31}P NMR and IR spectra. The treatment of $[\text{Fe}_2(\text{S}_2\text{C}_2\text{H}_4)(\text{CO})_2(\text{dppv})_2(\text{NO})]\text{BF}_4$ with NOBF_4 produced $\text{Fe}(\text{NO})_2(\text{dppv})$.²⁴

$[\text{Fe}_2(\text{S}_2\text{C}_2\text{H}_4)(\text{CO})_3(\text{dppv})(\text{PMe}_3)_2(\text{NO})]\text{BF}_4$, $[\text{I}(\text{CO})_3(\text{PMe}_3)_2]\text{BF}_4$. Onto a frozen solution of 0.206 g (0.26 mmol) of $[\text{I}(\text{CO})_3]\text{BF}_4$ in 10 mL of CH_2Cl_2 was distilled 1 mL of PMe_3 . The mixture was allowed to thaw at -78 °C and was warmed in an ice water bath for

1 min, followed by cooling again to -78 °C. The IR spectrum of the reaction mixture indicated $[\text{I}(\text{CO})_3(\text{PMe}_3)_2]\text{BF}_4$. The addition of 50 mL of hexanes to the reaction mixture yielded a dark brown oil that was dried in vacuo. IR spectra of the redissolved material contained traces of $[\text{I}(\text{CO})_2(\text{PMe}_3)]\text{BF}_4$, indicative of the thermal instability of $[\text{I}(\text{CO})_3(\text{PMe}_3)_2]\text{BF}_4$. ^{31}P NMR (CD_2Cl_2 , 0 °C), A, B, and C correspond to three isomers: δ 98.4 (d, $J_{\text{P-P}} = 48.3$, dppv A), 98.0 (d, $J_{\text{P-P}} = 44.3$, dppv B), 97.3 (d, $J_{\text{P-P}} = 39.7$, dppv C), 81.5 (d, $J_{\text{P-P}} = 48.9$, dppv A), 81.3 (d, $J_{\text{P-P}} = 45.8$, dppv B), 78.8 (d, $J_{\text{P-P}} = 38.4$, dppv C), 25.3, 17.8 (d, $J = 64.1$, PMe_3 C), 17.0 (d, $J = 62.5$, PMe_3 A), 10.0 (AB_q , $J = 292$, $J_{\text{AB}} = 245$, PMe_3 B), 6.4 (d, $J = 64.2$, PMe_3 C), 5.4 (d, $J = 65.6$, PMe_3 A).

Crystallization of $[\text{Fe}_2(\text{S}_2\text{C}_3\text{H}_6)(\text{CO})_3(\text{dppv})(\text{PMe}_3)_2(\text{NO})]\text{BF}_4$, $[\text{2}(\text{CO})_3(\text{PMe}_3)_2]\text{BF}_4$. Approximately 0.2 mL of PMe_3 was distilled onto a frozen solution of 0.070 g of $[\text{I}(\text{CO})_3]\text{BF}_4$ in 7 mL of CH_2Cl_2 . Aliquots briefly warmed (<2 min) to room temperature displayed an IR spectrum that indicated the presence of $[\text{2}(\text{CO})_3(\text{PMe}_3)_2(\text{NO})]\text{BF}_4$. IR (CH_2Cl_2): $\nu_{\text{CO}} = 2021, 1971, 1951; \nu_{\text{NO}} = 1721 \text{ cm}^{-1}$. NMR (CD_2Cl_2 , -20 °C), A, B, and C correspond to three isomers: δ 97.4 (d, $J_{\text{P-P}} = 34.2$, dppv A), 95.0 (d, $J_{\text{P-P}} = 28.6$, dppv B), 78.2 (d, $J_{\text{P-P}} = 38.2$, dppv A), 76.9 (d, $J_{\text{P-P}} = 29.0$, dppv B), 15.9 (d, $J_{\text{P-P}} = 71.6$, PMe_3 A), 15.2 (d, $J_{\text{P-P}} = 72.4$, PMe_3 C), 9.0 (AB_q , $J = 964.5$, $J_{\text{AB}} = 193$, PMe_3 B), 4.1 (d, $J_{\text{P-P}}$, PMe_3 A), 2.8 (d, $J_{\text{P-P}} = 71.9$, PMe_3 C). The dppv signals for isomer C are not reported because of overlap with isomer A's signals). The reaction mixture was thawed to -45 °C followed by transfer via cannula to a Schlenk tube cooled to -78 °C. This solution was layered with 50 mL of a 1/1 mixture of Et_2O and hexane and stored at -30 °C. After 1 week, red rhombs were visible.

Reaction of $[\text{I}(\text{CO})_3]$ with 1 equiv of PMe_3 . To a J. Young NMR tube was added a solution of 0.025 g (0.03 mmol) of $[\text{I}(\text{CO})_3]\text{BF}_4$ in 1 mL of CD_2Cl_2 . The solution was frozen in liquid nitrogen, and to it was added 0.3 mL of a 0.13 M solution of PMe_3 in CH_2Cl_2 . The tube was immediately capped, immersed in liquid nitrogen, and evacuated. The contents were allowed to warm and were monitored by NMR spectroscopy at various temperatures. At -38 °C, no reaction was observed. Upon warming to 0 °C, partial consumption of $[\text{I}(\text{CO})_3(\text{dppv})(\text{NO})]\text{BF}_4$ and nearly complete consumption of PMe_3 were accompanied by the growth of several peaks. These peaks were assigned to one major ("B") and two minor ("A" and "C") intermediates (see above spectra assignments). Upon warming to room temperature overnight, conversion of the remaining intermediate(s) to $[\text{I}(\text{CO})_2(\text{PMe}_3)]\text{BF}_4$ was observed.

$\text{NEt}_4[\text{Fe}_2(\text{S}_2\text{C}_2\text{H}_4)(\text{CN})_2(\text{CO})(\text{dppv})(\text{NO})]$. A solution of 0.503 g (0.63 mmol) of $[\text{I}(\text{CO})_3]\text{BF}_4$ in 30 mL of MeCN was cooled to -45 °C followed by treatment with a solution of 0.199 g (1.3 mmol) of NEt_4CN in 30 mL of MeCN, also cooled to -45 °C. The solution immediately darkened, and after 3 h, the dark brown solution was allowed to warm to room temperature followed by stirring overnight. After the solvent was removed in vacuo, the residue was extracted into 5 mL of CH_2Cl_2 , and the product was precipitated by the addition of 30 mL of Et_2O . IR (CH_2Cl_2): $\nu_{\text{CN}} = 2100, \nu_{\text{CO}} = 1923, \nu_{\text{NO}} = 1719$. ^{31}P NMR (CD_2Cl_2 , 20 °C): δ 96.1 (s, dppv). ^{31}P NMR (CD_2Cl_2 , -60 °C): δ 99.3 (d, $J_{\text{P-P}} = 22.4$, dppv), 94.1 (d, $J_{\text{P-P}} = 22.4$, dppv). ESI-MS: m/z 710.0 ($[\text{Fe}_2(\text{S}_2\text{C}_2\text{H}_4)(\text{CN})_2(\text{CO})(\text{dppv})(\text{NO})]^+$), 682.0 ($[\text{Fe}_2(\text{S}_2\text{C}_2\text{H}_4)(\text{CN})_2(\text{dppv})(\text{NO})]^+$). Suitable CHN analyses were not obtained.

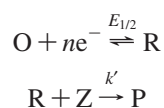
$[\text{Fe}_2(\text{S}_2\text{C}_2\text{H}_4)(\text{CO})(\text{CN})(\text{dppv})(\text{PMe}_3)(\text{NO})]\text{BF}_4$, $[\text{I}(\text{CO})(\text{CN})(\text{PMe}_3)]\text{BF}_4$. A solution of 0.221 g (0.26 mmol) of $[\text{I}(\text{CO})_2(\text{PMe}_3)]\text{BF}_4$ in 30 mL of CH_2Cl_2 was treated with a solution of 0.041 g (0.26 mmol) of NEt_4CN in 10 mL of MeCN. After 60 min, the dark-brown-colored reaction mixture was evaporated in vacuo, and the residue was extracted into 30 mL of toluene. The dark-red-colored extract was

(24) Guillaume, P.; Wah, H. L. K.; Postel, M. *Inorg. Chem.* **1991**, *30*, 1828–31.

concentrated, followed by dilution with 30 mL of hexanes to precipitate the product. Yield: 0.065 g (33%). $^1\text{H NMR}$ (d^8 -toluene): δ 8.5–6.7 (m, C_6H_5 and $\text{P}_2\text{C}_2\text{H}_2$), 2.1–1.6 (m, $\text{S}_2\text{C}_2\text{H}_4$), 1.26 (d, $J_{\text{P-H}} = 9.9$, 9H, PCH_3). $^{31}\text{P NMR}$ (CD_2Cl_2 , 20 °C): δ 95.3 (d, $J_{\text{P-P}} = 20.9$, dppv), 74.2 (d, $J_{\text{P-P}} = 24.5$, dppv), 7.9 (s, PMe_3). IR (CH_2Cl_2): $\nu_{\text{CN}} = 2096$, $\nu_{\text{CO}} = 1910$, $\nu_{\text{NO}} = 1734$. FD-MS: m/z 760 ($[\text{Fe}_2(\text{S}_2\text{C}_2\text{H}_4)(\text{CN})(\text{CO})(\text{dppv})(\text{PMe}_3)(\text{NO})]^+$). Anal. calcd (found) for $\text{C}_{33}\text{H}_{35}\text{Fe}_2\text{N}_2\text{O}_2\text{P}_3\text{S}_2$: C, 52.54 (52.13); H, 4.72 (4.64); N, 3.53 (3.68).

Relative Electrophilicity of $[\text{Fe}_2(\text{S}_2\text{C}_2\text{H}_4)(\text{CO})_3(\text{dppv})(\text{NO})]^+$. To a solution of 0.015 g (0.02 mmol) of $[\text{Fe}_2(\text{S}_2\text{C}_2\text{H}_4)(\text{CO})_3(\text{dppv})(\text{NO})]\text{BF}_4$ and 0.014 g (0.02 mmol) of $\text{Fe}_2(\text{S}_2\text{C}_2\text{H}_4)(\text{CO})_4(\text{dppv})$ in 5 mL of CH_2Cl_2 was added 0.5 mL of a 0.19 M solution of PMe_3 in CH_2Cl_2 . The reaction was monitored by IR spectroscopy over the course of 7 h, during which time the absorption bands for $[\text{I}(\text{CO})_3(\text{NO})]\text{BF}_4$ decayed and those for $[\text{I}(\text{CO})_3(\text{PMe}_3)(\text{NO})]\text{BF}_4$ increased. The bands for $\text{Fe}_2(\text{S}_2\text{C}_2\text{H}_4)(\text{CO})_4(\text{dppv})$ remained unchanged.

Semiquantitation of Catalytic Proton Reduction. An electron transfer followed by a fast catalytic reaction can be formulated by the following equations:



where k' is the rate constant for the reaction of reagent Z with the reduced species R to give product P. When the concentration of Z is large compared to the concentration of the catalyst and the potential sufficiently negative with respect to $E_{1/2}$, the catalytic current i_k is given by the following relation:¹⁵

$$i_k = nFAC_0\sqrt{k'DC_z}$$

where n is the number of electrons involved in the catalytic process, F the Faraday constant, A the area of the electrode, and D the diffusion coefficient for the catalyst. For graphs of i_k against $C_z^{1/2}$, the slope is $nFAC_0(k'D)^{1/2}$. The value for $AC_0D^{1/2}$ can be obtained

from the voltammetric peak current, i_p , of the catalyst in the absence of acid:

$$i_p = (2.69 \times 10^5)n^{3/2}AD^{1/2}C_0\nu^{1/2}$$

where ν is the potential scan rate.

X-Ray Crystallography. Crystals were mounted on a thin glass fiber using Paratone-N oil (Exxon). Data, collected at 198 K on a Siemens CCD diffractometer, were filtered to remove statistical outliers. The integration software (SAINT) was used to test for crystal decay as a bilinear function of X-ray exposure time and $\sin(\Theta)$. The data were solved using SHELXTL by direct methods; atomic positions were deduced from an E map or by an unweighted difference Fourier synthesis. H-atom U values were assigned as $1.2U_{\text{eq}}$ for adjacent C atoms. Non-H atoms were refined anisotropically. Successful convergence of the full-matrix least-squares refinement of F^2 was indicated by the maximum shift/error for the final cycle. The assignment of NO versus CO was tested by refining the cations with these ligands interchanged. Optimal refinements were found only for cases with the $\text{Fe}(\text{dppv})(\text{NO})$ centers. Structure refinement details of the discussed compounds are given in Table 4.

Acknowledgment. This work was supported by the National Institutes of Health. We thank Terésa Prussak-Wieckowska for assistance with the crystallographic analyses. M.T.O. thanks the NIH Chemistry–Biology Interface Training Program for a fellowship. We thank the CNRS-UIUC cooperation program for support for F.G. during his time at UIUC. Dr. M. Nilges recorded and simulated the EPR spectrum of $[\text{Fe}_2(\text{S}_2\text{C}_2\text{H}_4)(\text{CO})(\text{NO})(\text{dppv})_2]$.

Supporting Information Available: X-ray crystallographic data and additional spectroscopic and synthetic details. This material is available free of charge via the Internet at <http://pubs.acs.org>.

IC801542W